Title

Growth, CO2 Consumption, and H2 Production of Anabaena variabilis ATCC 29413-U under Different Irradiances and CO2 Concentrations

Journal

Journal of Applied Microbiology, 104

Authors

Berberoglu, Halil
Barra, Natasha
Pilon, Laurent
et al.

Publication Date

2008

Peer reviewed

Growth, CO_2 Consumption, and H_2 Production of *Anabaena variabilis* ATCC 29413-U under Different Irradiances and CO_2 Concentrations

Halil Berberoğlu[†], Natasha Barra[†], Laurent Pilon[†,§], and Jenny Jay[*]

[†]Mechanical and Aerospace Engineering Department

Henry Samueli School of Engineering and Applied Science

University of California, Los Angeles - Los Angeles, CA 90095, USA

[*]Civil and Environmental Engineering Department

Henry Samueli School of Engineering and Applied Science

University of California Los Angeles - Los Angeles, CA 90095, USA

[§] Corresponding author. Phone: +1 (310)-206-5598, Fax: +1 (310)-206-4830

E-mail: pilon@seas.ucla.edu

May 31, 2007

Abstract

Aims: The objective of this study is to develop kinetic models based on batch experiments describing the growth, CO_2 consumption, and H_2 production of *Anabaena variabilis* ATCC 29413-U^{TM} as functions of irradiance and CO_2 concentration.

Methods and Results: A parametric experimental study is performed for irradiances from 1120 to 16100 lux and for initial CO_2 mole fractions from 0.03 to 0.20 in argon at pH 7.0 $\pm$ 0.4 with nitrate in the medium. Kinetic models are successfully developed based on the Monod model and on a novel scaling analysis employing the CO_2 consumption half-time as the time scale.

Conclusions: Monod models predict the growth, CO_2 consumption, and O_2 production within 30%. Moreover, the CO_2 consumption half-time is an appropriate time scale for analyzing all experimental data. In addition, the optimum initial CO_2 mole fraction is 0.05 for maximum growth and CO_2 consumption rates. Finally, the saturation irradiance is determined to be 5,170 lux for CO_2 consumption and growth whereas, the maximum H_2 production rate occurs around 10,000 lux.

Significance and Impact: The study presents kinetic models predicting the growth, CO_2 consumption, and H_2 production of *A.variabilis*. The experimental and scaling analysis methods can be generalized to other microorganisms.

Nomenclature

C	volumetric mass concentration, kg/m^3
C_{TOT}	molar concentration of total dissolved inorganic carbon, kmol/m^3
$E_{ext,\lambda}$	spectral extinction cross-section, m^2/kg dry cell
$E_{ext,PAR}$	average extinction cross-section over the PAR, m^2/kg dry cell
G	local irradiance, lux
G_{av}	average irradiance within the culture in the spectral range from 400 to 700 nm, lux
G_{in}	total incident irradiance in the spectral range from 400 to 700 nm, lux
K_C	half-saturation constant for dissolved inorganic carbon, kmol/m^3
K_G	half-saturation constant for light, lux
K_I	inhibition constant for dissolved inorganic carbon, kmol/m^3
L	depth of the cyanobacteria suspension in the vial, m
OD	optical density
t	time, h
$t_{1/2}$	half-time, h
X	cyanobacteria concentration, kg dry cell/m^3
$X_{avg,\Delta t}$	average cyanobacteria concentration in the time interval Δt, kg dry cell/m^3
x	mole fraction
$\mathrm{Y}_{X/C}$	biomass yield based on carbon, kg dry cell/kmol C
Y_{X/CO_2}	biomass yield based on CO_2, kg dry cell/kg CO_2
$\mathrm{Y}_{O_2/X}$	O_2 yield based on biomass, kg O_2/kg dry cell
z	location in the cyanobacteria suspension measured from the liquid surface, m

Greek symbols

α	exponential constant
β	slope of half-time versus initial CO_2 mole fraction in the gas phase, h
$\mu_{\Delta t}$	specific growth rate in the time interval Δt, 1/h
μ_{avg}	average specific growth rate, 1/h
μ_{max}	maximum specific growth rate, 1/h

ψ_{CO_2}	average specific CO_2 uptake rate, kg CO_2/kg dry cell/h

Subscripts

CO_2	refers to carbon dioxide
g	refers to gas phase
H_2	refers to hydrogen
i	refers to a gas species
L	refers to liquid phase
max	refers to the maximum amount of a gas species produced by the cyanobacteria
O_2	refers to oxygen
o	refers to initial conditions

1 Introduction

Increased amounts of greenhouse gas emissions as well as the exhaustion of easily accessible fossil fuel resources are calling for effective CO_2 mitigation technologies and clean and renewable energy sources. Hydrogen, for use in fuel cells, is considered to be an attractive alternative fuel since water vapor is the only byproduct from its reaction with oxygen. Hydrogen production by cultivation of cyanobacteria in photobioreactors offers a clean and renewable alternative to thermochemical or electrolytic hydrogen production technologies with the added advantage of CO_2 mitigation. In particular, *Anabaena variabilis* is a cyanobacterium capable of mitigating CO_2 and producing H_2. The objective of this study is to experimentally investigate the CO_2 mitigation, growth, and H_2 production of *A.variabilis* ATCC 29413-U^{TM} in BG-11 medium under atmosphere containing argon and CO_2. Parameters investigated are the irradiance and the initial CO_2 mole fraction in the gas phase.

The cyanobacterium *Anabaena variabilis* is a photosynthetic prokaryote listed among the potential candidates for hydrogen production (Pinto, Troshina and Lindblad 2002), whose genome sequence has been completed (of Energy Accessed on: April 19, 2007). Moreover, *A.variabilis* and its mutants are of great interest in research as hydrogen producers (Yoon, Sim, Kim and Park, 2002; Hansel and Lindblad, 1998; Pinto et al., 2002; Tsygankov, Serebryakova, Rao and Hall, 1998; Borodin, Tsygankov, Rao and Hall, 2000; Happe, Schutz and Bohme, 2000). *A.variabilis* utilizes light energy in the spectral range from 400 to 700 nm, known as photosynthetically active radiation (PAR), and consumes CO_2 to produce biomass, oxygen, and hydrogen. The reader is referred to Refs. (Das and Veziroglu, 2001; Benemann, 2000; Prince and Kheshgi, 2005; Pinto et al., 2002; Madamwar, Garg and Shah, 2000) for detailed reviews of photobiological hydrogen production. In brief, *A.variabilis* utilizes water as its electron donor (Prince and Kheshgi, 2005) and produces hydrogen mainly using nitrogenase enzyme (Madamwar et al., 2000). The primary role of nitrogenase is to reduce nitrogen to ammonia during nitrogen fixation (Das and Veziroglu, 2001). H_2 is produced as a by product of this reaction (Das and Veziroglu, 2001). In the absence of molecular nitrogen, nitrogenase will reduce protons and catalyze the production of H_2 provided reductants and ATP are present (Das and Veziroglu, 2001). Nitrogenase enzyme is located

in special cells called heterocysts, which protect nitrogenase from O_2 inhibition (Tsygankov et al., 1998). However, at dissolved O_2 concentrations higher than 50 μM, the produced H_2 is consumed by *A.variabilis* in a reaction catalyzed by the enzyme "uptake" hydrogenase (Tsygankov et al., 1998), thus reducing the net H_2 production rate (Tsygankov et al., 1998). Finally, *A.variabilis* also possesses bi-directional hydrogenases located at the cytoplasmic membrane (Madamwar et al., 2000). However, unlike nitrogenase, these enzymes are not well protected from oxygen and their functioning is inhibited at relatively low O_2 concentrations (Benemann, 2000).

Table 1 summarizes previous studies on H_2 production by *A.variabilis*. It indicates the strain used, the gas phase composition, irradiance and the medium used during growth and H_2 production stages, as well as the specific growth, CO_2 consumption, and H_2 production rates. Briefly, Tsygankov et al. (1998) and Sveshnikov, Sveshnikova, Rao and Hall (1997) studied the hydrogen production by *Anabaena variabilis* ATCC 29413 and by its mutant PK84, lacking the hydrogen uptake metabolism. On the other hand, Markov, Lichtl, Rao and Hall (1993) proposed a two stage photobioreactor alternating between (i) growth and (ii) H_2 production phases for attaining high H_2 production rates. During the growth phase cyanobacteria fix CO_2 and nitrogen from the atmosphere to grow and produce photosynthates. In the H_2 production phase, they utilize the photosynthates to produce H_2. In addition, Yoon et al. (2002) used a two stage batch process and suggested an improvement on the first stage by incorporating nitrate in the growth medium for faster growth of *A.variabilis*. As opposed to using a two stage photobioreactor, Markov, Weaver and Seibert (1997b) demonstrated a single stage photobioreactor using *A.variabilis* PK-84 in a helical photobioreactor. More recently, Tsygankov, Fedorov, Kosourov and Rao (2002) demonstrated a single stage photobioreactor operation for H_2 production using *A.variabilis* PK-84 in an outdoor photobioreactor similar to that of Markov et al. (1997b).

Most previous studies using *A.variabilis* have used a two stage photobioreactor with relatively limited ranges of CO_2 concentrations and light irradiance. In addition, to the best of our knowledge, there has been no reported study simultaneously varying irradiance and the initial CO_2 mole fraction in the gas phase to quantitatively assess the CO_2 mitigation, growth, and H_2 production of *A.variabilis* in a single stage process. The objectives of this work are (i) to develop kinetic

models based on batch experiments describing the growth, CO_2 consumption, and H_2 production of *Anabaena variabilis* ATCC 29413-U^{TM} as functions of irradiance and CO_2 concentration and (ii) to provide recommendations on the optimum irradiance and the gas phase CO_2 mole fraction for achieving rapid growth, high CO_2 uptake, and H_2 production rates.

2 Materials and Methods

A cyanobacterial suspension was prepared from a 7 day old culture. The microorganism concentration denoted by X was adjusted to 0.02 kg dry cell/m^3 by diluting the culture with fresh medium and was confirmed by monitoring the optical density (OD). Then, 60 mL of the prepared suspension was dispensed in 160 mL serum vials. The vials were sealed with butyl rubber septa, crimped, and flushed through the septa with industrial grade argon, sterilized with 0.2 μm pore size syringe filter, for 10 minutes with a needle submerged in the liquid phase. The initial CO_2 mole fraction in the head-space, denoted by $x_{CO_2,g,o}$, was set at 0.03, 0.04, 0.08, 0.15, and 0.20. This was achieved first by adjusting the gauge pressure in the vials to -7.09, -10.13, -20.27, -30.40, and -40.53 kPa, respectively. Then, 7, 10, 20, 30, and 40 mL of industrial grade CO_2 were injected into the vials, respectively, through a 0.2 μm pore size syringe filter. The vials were shaken until the head-space pressure stabilized indicating that both the partitioning of CO_2 between the gas and liquid phases and the dissolution of CO_2 in water were at equilibrium. Finally, the head-space was sampled to measure the initial CO_2 mole fraction. Each vial was prepared in duplicates. The vials were placed horizontally on an orbital shaker (model ZD-9556 by Madell Technology Group, USA) and stirred continuously at 115 rpm throughout the duration of the experiments. Continuous illumination was provided from the top of the orbital shaker. The transparent glass vials could be approximated to a cylindrical tube of diameter 50 mm, of height 80 mm, and of wall thickness 2 mm. The illuminated surface area of each vial was 40×10^{-4} m^2. The irradiance, defined as the total radiant flux of visible light from 400 to 700 nm incident on a vial from the hemisphere above it, ranged from 1,120 to 16,100 lux. Note that for the lamps used in the experiments 1 lux of irradiance was equivalent to 3×10^{-3} W/m^2 and 14×10^{-3} μmol/m^2/s in the PAR.

Throughout the experiments CO_2, H_2, and O_2 concentrations in the head-space as well as the

cyanobacteria concentration and pH in the liquid phase were continually monitored. In addition, the temperature and pressure of the vials were measured in order to convert the molar fractions of gas species into volumetric mass concentrations. The irradiance incident on individual vials was recorded. Details of the experimental setup and procedures are given in the following sections.

Cyanobacteria Culture and Concentration Measurements

Anabaena variabilis ATCC 29413-U^{TM} was purchased from the American Type Culture Collection (ATCC) and received in freeze dried form. The culture was activated with 10 mL of sterilized milli-Q water. It was cultivated and transferred weekly in ATCC medium 616 with air-CO_2 mixture in the head-space with an initial mole fraction of CO_2 of 0.05. One liter of ATCC medium 616 contained 1.5 g $NaNO_3$, 0.04 g K_2HPO_4, 0.075 g $MgSO_4 \cdot 7H_2O$, 0.036 g $CaCl_2 \cdot 2H_2O$, 6.0 mg citric acid, 6.0 mg ferric ammonium citrate, 0.02 g Na_2CO_3, 1.0 mg EDTA, and 1.0 mL of trace metal mix A5. One liter of trace metal mix A5 contains 2.86 g H_3BO_3, 1.81 g $MnCl_2 \cdot 4H_2O$, 0.222 g $ZnSO_4 \cdot 7H_2O$, 0.39 g $Na_2MoO_4 \cdot 2H_2O$, 0.079 g $CuSO_4 \cdot 5H_2O$, 49.4 $mg\ Co(NO_3)_3 \cdot 6H_2O$. The pH of the medium was adjusted to be 7.3 by adding 1M HCl and/or 1M NaOH. Then, 20 mL of HEPES buffer solution at pH 7.3 was added to one liter of medium. Finally, the medium was autoclaved at 121^oC for 40 minutes.

The cyanobacteria concentration X was determined by sampling 1 mL of bacteria suspension from the vials and measuring the optical density (OD). A calibration curve was created by measuring both the dry cell weight of a cyanobacteria suspension and the corresponding OD. First, the OD of the cyanobacteria was measured in disposable polystyrene cuvettes with light path of 10 mm at 683 nm (Yoon et al., 2002) using a UV-Vis spectrophotometer (Cary-3E by Varian, USA). Then, the bacteria suspension was filtered through mixed cellulose filter membranes with 0.45 μm pore size (HAWP-04700 by Millipore, USA) and dried at 85^oC over night. The dried filters were weighed immediately after being taken out of the oven on a precision balance (model AT261 by Delta Range Factory, USA) with a precision of 0.01 mg. The calibration curve for OD was generated by using 14 different bacteria concentrations ranging from 0.04 to 0.32 kg dry cell/m^3. The

relation between OD and bacteria concentration is linear for the OD range from 0 to 1.2 and one unit of OD corresponds to 0.274 kg dry cell/m^3.

Temperature, Pressure, and pH

The temperature of the vials was measured with a thermocouple (Dual Thermometer, Fisher Scientific, USA). The heat from the high intensity fluorescent bulbs was removed by convective cooling using a fan to maintain a steady-state temperature of 24 ± 1^oC throughout the duration of the experiments. The head-space pressure was monitored with a digital gauge pressure sensor (model PX26-005GV by Omega Heater Company, USA) connected to a digital meter (model DP25B-S by Omega Heater Company, USA). Finally, the pH of the medium was measured with a digital pH probe (model Basic AB Plus, Fisher Scientific, USA).

Lighting and Light Analysis

The irradiance incident on the vials G_{in} was provided by fluorescent light bulbs (Ecologic by Sylvania, USA and Fluorex by Lights of America, USA) and varied by changing the number of bulbs. The spectral irradiance of these bulbs were measured with a spectrophotometer (model USB2000, Ocean Optics) connected to a cosine collector over the spectral range from 350 to 750 nm. The spectral irradiance of the light bulbs G_λ, normalized with its maximum value G_{max} at 540 nm, along with the reported cyanobacterial absorption coefficient κ_λ (Merzlyak and Naqvi, 2000), normalized with its maximum value κ_{max}, are presented in Figure 1. The irradiance incident on the vials was measured with both a light meter (Fisherbrand Tracable Meter by Fisher Scientific, USA) and a quantum sensor (LI-COR, Model LI-190SL, LI-COR Inc., USA). The total irradiance on each vial was measured individually in the photosynthetically active radiation (PAR), i.e., within the spectral range from 400 to 700 nm, . Due to experimental difficulties in achieving the exact same irradiance for all vials, five different irradiance ranges were explored namely, 1120-1265 lux, 1680-2430 lux, 3950-4600 lux, 7000-8700 lux, and 14,700-16,100 lux.

Gas Analysis

The gas analysis was carried out every 24 hours by sampling 500 μL of head-space volume of the vials. The concentrations of CO_2, H_2, and O_2 in the head-space were measured with a gas chromatographer (HP-5890, Hewlett Packard) equipped with a packed column (Carboxen-1000 by Supelco, USA) and a thermal conductivity detector (TCD). The gas chromatographer output was processed with an integrator (HP-3395, Hewlett Packard, USA). Throughout the gas analysis, the injector and detector temperatures were maintained at 120^oC. During the H_2 and O_2, analysis argon was used as the carrier gas and the oven temperature was maintained at 35^oC. The retention times for H_2 and O_2 were found to be 2.1 and 7.5 minutes, respectively. On the other hand, during the CO_2 analysis, Helium was used as the carrier gas and the oven temperature was maintained at 255^oC. The retention time for CO_2 was then 4.9 minutes. Calibration curves for the TCD response were prepared at seven different known gas concentrations from 16×10^{-6} to 3.2×10^{-3} kg/m^3 for H_2, from 25.6×10^{-3} to $1{,}314\times10^{-3}$ kg/m^3 for O_2, and from 3.96×10^{-3} to 352×10^{-3} kg/m^3 for CO_2. All calibration curves were linear within these gas concentration ranges. During the experiments, peak heights were recorded and correlated with the corresponding moles of gas using the respective calibration curves.

3 Results

The experimental parameters used in the study along with the experimental labels are summarized in Table 2. In brief, the initial CO_2 mole fraction in the head-space, $x_{CO_2,g,o}$, varied from 0.03 to 0.20 while the irradiance G varies from 1,120 to 16,100 lux. Pressure, temperature, and pH were maintained at 1 ± 0.1 atm., 24 ± 1^oC, and 7.0 ± 0.4, respectively. In order to develop semi-empirical models for CO_2 consumption, growth, H_2, and O_2 production by *A.variabilis* ATCC 29413 using the experimental data, the following assumptions are made:

1. The concentration of gases in each phase and the concentration of cyanobacteria in the liquid phase are uniform within a given vial, due to vigorous mixing provided by the orbital shaker.

2. The Damkohler number, defined as the ratio of the reaction rate to the mass transfer rate

(Smith, McCarthy and Kitanidis, 1998), associated with the experimental setup is on the order of 10^{-4}. Therefore, metabolic reactions of the cyanobacteria are not mass transfer limited (Smith et al., 1998).

3. The gas species in the liquid and gas phases are at quasi-equilibrium at all times.

4. *A.variabilis* both consumes and produces CO_2, O_2, and H_2. Therefore, the reported gas phase concentration of species correspond to the net consumed or produced quantities.

5. The only parameters affecting the bacterial growth and product formation are the CO_2 concentration and the irradiance G. The supply of other nutrients such as minerals and nitrate are assumed to be unlimited in the growth medium.

6. Given the pH range, the effect of buffer capacity on the growth rate is assumed to be negligible compared with the effects of CO_2 concentration and local irradiance.

7. The death of microorganisms is neglected the time frame of the experiments.

Kinetic Modeling

During the growth phase, the time rate of change of microorganism concentration X can be written as (Dunn, Heinzle, Ingham and Prenosil, 2003),

$$\frac{dX}{dt} = \mu X \tag{1}$$

where μ is the specific growth rate of the cyanobacteria expressed in s^{-1}. In this study it is assumed to be a function of (a) the average available irradiance denoted by G_{av} and (b) the concentration of total dissolved inorganic carbon within the cyanobacterial suspension denoted by C_{TOT}. The specific growth rate has been modeled using the Monod model taking into account (i) light saturation, (ii) CO_2 saturation, and (iii) CO_2 inhibition as (Asenjo and Merchuk, 1995),

$$\mu = \mu_{max} \left(\frac{G_{av}}{G_{av} + K_G} \right) \left(\frac{C_{TOT}}{K_C + C_{TOT} + C_{TOT}^2 / K_I} \right) \tag{2}$$

where μ_{max} is the maximum specific growth rate, K_G is the half-saturation constant for light, K_C and K_I are the half-saturation and the inhibition constants for dissolved inorganic carbon, respectively. First the spectral and local irradiance $G_\lambda(z)$ within the suspension is estimated using Beer-Lambert's law as,

$$G_\lambda(z) = G_{\lambda,in} exp(-E_{ext,\lambda} X z) \tag{3}$$

where $G_{\lambda,in}$ is the spectral irradiance incident on the vials, z is the distance from the top surface of the suspension, X is the microorganism concentration in kg dry cell/m^3, $E_{ext,\lambda}$ is the spectral extinction cross-section of *A.variabilis* at wavelength λ. Note that $E_{ext,\lambda}$ varies by less than 4% over the PAR and is assumed to be constant and equal to $E_{ext,PAR}$ =350 m^2/kg dry cell (Berberoğlu and Pilon, 2007). Then, the available irradiance G_{av} can be estimated by averaging the local irradiance over the depth of the culture L as,

$$G_{av} = \frac{1}{L}\int_0^L G(z)dz \qquad \text{where} \qquad G(z) = G_{in} exp(-E_{ext,PAR} X z) \tag{4}$$

Experimentally L is equal to 0.02 m.

Finally, C_{TOT} is the total dissolved inorganic carbon concentration in the liquid phase expressed in kmol/m^3. It depends on the pH of the medium and on the molar fraction of CO_2 in the gas phase $x_{CO_2,g}$ and can be written as (Benjamin, 2002),

$$C_{TOT} = 10^{-1.5} x_{CO_2,g} + \left(\frac{10^{-7.8}}{10^{-pH}}\right) x_{CO_2,g} + \left(\frac{10^{-28.1}}{10^{-2pH}}\right) x_{CO_2,g} \tag{5}$$

where the three terms on the right hand side correspond to $H_2CO_3^*$, HCO_3^-, and CO_3^{2-} concentrations in the liquid phase, respectively.

The values of the parameters μ_{max}, K_G, K_C, and K_I in Equation (2) are estimated by minimizing the root mean square error between the experimentally measured cyanobacteria concentrations and the model predictions obtained by integrating Equations (1) and (2). The associated parameters along with those reported by Erickson, Curless and Lee (1987) for the cyanobacteria *Spirulina platensis* are summarized in Table 3. Figure 2(a) compares the cyanobacteria concentrations measured experimentally with the model predictions. It indicates that the model predicts the experimental data for microorganism concentration within 30%.

Moreover, assuming that the biomass yield based on consumed carbon and denoted by $Y_{X/C}$ is constant, as assumed by Erickson et al. (1987), the total dissolved inorganic carbon concentration can be modeled as (Dunn et al., 2003),

$$\frac{dC_{TOT}}{dt} = -\frac{\mu}{Y_{X/C}}X \tag{6}$$

The yield $Y_{X/C}$ can be expressed in terms of the biomass yield based on consumed CO_2 denoted by Y_{X/CO_2} as $Y_{X/C} = M_{CO_2}Y_{X/CO_2}$ where M_{CO_2} is the molecular weight of CO_2 equal to 44 kg/kmol. The value of Y_{X/CO_2} for each experiment is given in Table 2. The value of $Y_{X/C}$ used in this study is the average value obtained across experiments which is equal to 24.96 kg dry cell/kmol C. Figure 2(b) compares C_{TOT} obtained using Equation (5) and the measured pH and $x_{CO_2,g}$ with the value predicted by integrating Equation (6). It shows that the model predicts the experimental data within 30%.

Furthermore, assuming that one mole of O_2 is evolved per mole of CO_2 consumed, the total oxygen concentration in the vial can be computed as,

$$\frac{dC_{O_2}}{dt} = Y_{O_2/X}\mu X \tag{7}$$

where $Y_{O_2/X}$ is the O_2 yield based on biomass and equal to 1.28 kg O_2/kg dry cell. It is expressed as $M_{O_2}/Y_{X/C}$ where M_{O_2} is the molecular weight of O_2 equal to 32 kg/kmol. Figure 2(c) compares the total O_2 concentration measured experimentally with that predicted by integrating Equation (7). It indicates that the experimental data for C_{O_2} falls within 30% of model's predictions.

Finally, models similar to Equations (6) and (7) were applied to the H_2 concentration in the headspace measured as a function of time. However, yield coefficients could not be obtained to model the experimental data within 30%.

Scaling Analysis

The models described in the previous section depend on quantities such as G_{av} and C_{TOT} that are not directly measurable. They are typically kept constant by using either a chemostat (Erickson et

al., 1987) or a turbidostat (Goldman, Oswald and Jenkins, 1974). However, construction and operation of these devices are relatively expensive and experimentally more challenging than the vial experiments performed in this study. Moreover, a number of assumptions had to be made to estimate the parameters of the kinetic models. Specifically, G_{av} was estimated using Beer-Lambert's law which does not take into account in-scattering by the microorganisms and can lead to errors as high as 30% in estimating the local irradiance $G_\lambda(z)$ (Berberoğlu, Yin and Pilon, 2007). Moreover, the growth rates of the microorganisms were assumed to be independent of pH which varied between 7.0 ± 0.4 during the course of the experiments. Furthermore, the average yields $Y_{X/C}$ and $Y_{O_2/X}$ were assumed to be constant in modeling the CO_2 consumption and O_2 production. Finally, modeling H_2 production with the approach above gave poor results. Therefore, as an alternative to the kinetic models described above, a novel scaling analysis is presented for analyzing the data based on the directly measurable molar fraction $x_{CO_2,g,o}$ and incident irradiance G_{in} while G_{av} and C_{TOT} are allowed to vary with time.

CO_2 Consumption

Figure 3(a) shows the evolution of the CO_2 molar fraction $x_{CO_2,g}$ in the head-space as a function of time t, normalized with the initial CO_2 mole fraction $x_{CO_2,g,o}$ for different combinations of the total incident irradiance G_{in} and $x_{CO_2,g,o}$. It indicates that $x_{CO_2,g}$ decreases monotonically with increasing time. First, the half-time, denoted by $t_{1/2}$, is defined as the time required for the CO_2 mole fraction in the gas phase to decrease to half of its initial value. Normalizing the time by the half-time and plotting the dimensionless variables $x_{CO_2,g}/x_{CO_2,g,o}$ versus $t/t_{1/2}$, collapses all the data points to a single line as shown in Figure 3(b). This indicates that the CO_2 consumption half time is an appropriate time scale for comparing CO_2 consumption under different conditions. Performing a linear regression analysis of the data yields,

$$\frac{x_{CO_2,g}}{x_{CO_2,g,o}} = 1 - 0.5\left(\frac{t}{t_{1/2}}\right)^{1.2} \tag{8}$$

with a correlation coefficient $R^2 = 0.94$. Equation (8) also indicates that $x_{CO_2,g}$ vanishes at time $t = 1.8t_{1/2}$.

Moreover, the half-time $t_{1/2}$ is a function of both the initial CO_2 mole fraction and the irradiance G_{in}. Figure 4(a) shows $t_{1/2}$ as a function of $x_{CO_2,g,o}$ for different values of G_{in}. It indicates that $t_{1/2}$ increases linearly with $x_{CO_2,g,o}$ for a given G_{in}, i.e., $t_{1/2} = \beta(G_{in})x_{CO_2,g,o}$, where the slope $\beta(G_{in})$ is expressed in hours and plotted in Figure 4(b). Two regimes can be identified. In the first regime, $\beta(G_{in})$ decreases linearly with G_{in} according to $\beta(G_{in}) = 1900 - 0.3G_{in}$. In the second regime, $\beta(G_{in})$ does not vary appreciably with G_{in} and has the approximate value of 350 hours. Figure 4(b) indicates that transition between the two regimes occurs around $G_{in} = 5,170$ lux. Therefore, the half-time $t_{1/2}$ can be expressed as,

$$\begin{aligned} t_{1/2} &= (1900 - 0.3G_{in})x_{CO_2,g,o} \qquad \text{for} \quad G_{in} \leq 5,170 \quad \text{lux} \\ t_{1/2} &= 350x_{CO_2,g,o} \qquad\qquad\qquad\quad \text{for} \quad G_{in} > 5,170 \quad \text{lux} \end{aligned} \tag{9}$$

Alternatively, the relationship between β and G_{in} can be approximated with an exponential decay function as $\beta(G_{in}) = 350 + 1300\text{exp}(9 \times 10^{-8}G_{in}^2)$.

Furthermore, Figure 5(a) compares the values of experimentally determined $t_{1/2}$ with those predicted by Equation (9). With the exception of one outlier, all the experimentally determined half-times lie within $\pm$ 20 hours of the predictions by Equation (9). The experimental values of $t_{1/2}$ and t_d are summarized in Table 2 for each test.

In addition, Figure 5(b) shows the medium pH as a function of the dimensionless time $t/t_{1/2}$ for all runs. It shows that the medium pH increases as the CO_2 is consumed by the microorganisms. It also indicates that the pH changes also scale well with the time scale $t_{1/2}$.

Cyanobacterial Growth

Figures 6(a) and (b) show the normalized concentration of *A.variabilis*, X/X_o, versus time t for all irradiances and for $x_{CO_2,g,o} = 0.08$ and 0.15, respectively. The initial cyanobacteria concentration X_o is equal to 0.02 kg dry cell/m^3 in all cases. Figure 6 establishes that for a given $x_{CO_2,g,o}$, increasing the irradiance increases the growth rate of *A.variabilis*. Moreover, for a given irradiance G_{in} within the values tested, decreasing the initial CO_2 mole fraction increases the growth rate. Thus, the effects of G_{in} and $x_{CO_2,g,o}$ on cyanobacterial growth seem to be coupled.

Here also, scaling the time with the half-time $t_{1/2}$ collapses the growth curves for different irradiances onto a single line as shown in Figures 6(c) and (d) for $x_{CO_2,g,o} = 0.08$ and 0.15, respectively. Therefore, the half-time $t_{1/2}$ correctly captures the time scale of the biological processes for CO_2 consumption and bacterial growth. In addition, the cyanobacterial growth is exponential and the cyanobacteria concentration $X(t)$ at time t can be expressed as,

$$\frac{X(t)}{X_o} = \exp\left(\frac{\alpha}{t_{1/2}}t\right) \tag{10}$$

where α is a constant depending on $x_{CO_2,g,o}$ and determined experimentally. Figure 7 shows its evolution as a function of $x_{CO_2,g,o}$ varying between 0.03 and 0.20. The relationship can be expressed as,

$$\alpha = 4x_{CO_2,g,o}^{0.35} \tag{11}$$

with a correlation coefficient R^2=0.93. Note that the evolution of $X(t)$ as a function of the irradiance G_{in} and $x_{CO_2,g,o}$ is accounted for through the half-time $t_{1/2}$ given by Equation (9).

Moreover, the average specific growth rate, denoted by μ_{avg}, is the arithmetic mean of the specific growth rates, denoted by $\mu_{\Delta t}$ and determined in the time interval Δt during the exponential growth phase of *A.variabilis* according to (Yoon et al., 2002),

$$\mu_{\Delta t} = \frac{\Delta X}{\Delta t}\frac{1}{X_{avg,\Delta t}} \tag{12}$$

where $X_{avg,\Delta t}$ is the arithmetic mean of the cyanobacteria concentration during that time interval Δt. The values of μ_{avg} computed for all parameters are summarized in Table 2. Figure 8(a) presents the variation of the average specific growth rate of *A.variabilis* denoted by μ_{avg} and expressed in h^{-1}, as a function of $x_{CO_2,g,o}$ for all irradiances. The error bars indicate the standard error that is the ratio of the standard deviation to the square root of the number of samples.

Furthermore, the average specific CO_2 uptake rate, denoted by ψ_{CO_2} and expressed in kg/kg dry cell/h, is computed using the same method as that used by Yoon et al. (2002),

$$\psi_{CO_2} = \frac{\mu_{avg}}{Y_{X/CO_2}} \tag{13}$$

where Y_{X/CO_2} is the biomass yield based on consumed CO_2 expressed in kg dry cell/kg of CO_2. It is computed as the ratio of the final mass of cyanobacteria produced to the total mass of CO_2

injected into the vials. The values of ψ_{CO_2} computed for all parameters are also summarized in Table 2. Figure 8(b) shows the variation of ψ_{CO_2} as a function of $x_{CO_2,g,o}$ for all irradiances.

Hydrogen and Oxygen Productions

Figure 9(a) shows the concentration of hydrogen measured in the head-space as a function of the dimensionless time $t/t_{1/2}$ for all runs. It indicates that the maximum hydrogen concentration is achieved at high irradiance. Moreover, the concentration of hydrogen accumulated in the head-space normalized with its maximum value $C_{H_2,g,max}$ as a function of dimensionless time $t/t_{1/2}$ for irradiance larger than 7,000 lux is shown in Figure 9(b). It establishes that $C_{H_2,g}/C_{H_2,g,max}$ varies exponentially with $t/t_{1/2}$ and can be expressed as,

$$\frac{C_{H_2,g}(t)}{C_{H_2,g,max}} = \exp\left[4.45\left(\frac{t}{t_{1/2}}\right) - 6.1\right] \tag{14}$$

Similarly, Figures 10(a) and (b) show the oxygen concentration and the normalized oxygen concentration with its maximum value, respectively, as functions of the dimensionless time $t/t_{1/2}$ for all runs. Figure 10(b) indicates that the normalized oxygen concentration varies exponentially with $t/t_{1/2}$ according to,

$$\frac{C_{O_2,g}(t)}{C_{O_2,g,max}} = \exp\left[2.25\left(\frac{t}{t_{1/2}}\right) - 3.5\right] \tag{15}$$

In order to use Equations (14) and (15) to determine the evolution of oxygen and hydrogen concentrations, the maximum concentrations $C_{O_2,g,max}$ and $C_{H_2,g,max}$ must be expressed in terms of the initial CO_2 mole fraction $x_{CO_2,g,o}$ and irradiance G. Figure 11 shows that $C_{O_2,g,max}$ is independent of irradiance and varies linearly with $x_{CO_2,g,o}$ according to,

$$C_{O_2,g,max} = 3.45 x_{CO_2,g,o} \tag{16}$$

with a correlation coefficient $R^2 = 0.94$. This demonstrates that the oxygen yield of *A.variabilis*, i.e., the mass of O_2 produced per mass of CO_2 consumed, was constant for the parameters explored.

Figure 12(a) shows $C_{H_2,g,max}$ as a function of both irradiance and of the initial CO_2 mole fraction. It indicates that within the parameter ranges explored, the optimum irradiance for maximum

H_2 production was around 10,000 lux. Figure 12(b) shows $C_{H_2,g,max}$ as a function of $x_{CO_2,g,o}$ for irradiances larger than 7,000 lux for which H_2 production is the largest. It indicates that $C_{H_2,g,max}$ increases with increasing $x_{CO_2,g,o}$. As a first order approximation, the relationship between $C_{H_2,g,max}$ and $x_{CO_2,g,o}$ can be written as,

$$C_{H_2,g,max} = 1.50 \times 10^{-2} x_{CO_2,g,o} - 3.75 \times 10^{-4} \quad \text{for} \quad G \geq 7,000 \quad \text{lux} \tag{17}$$

with a correlation coefficient R^2 of 0.75.

4 Discussion

Kinetic models describing the cyanobacterial growth, carbon uptake, and O_2 production depend on the specific growth rate μ which is a function of the instantaneous available irradiance G_{av} and total dissolved inorganic carbon concentration C_{TOT}. In an earlier study, Badger and Andrews (1982) suggested that both $H_2CO_3^*$ and HCO_3^- can act as substrate for cyanobacteria. Furthermore, Goldman et al. (1974) used C_{TOT} given by Equation (5) in the Monod model to successfully predict algal growth in carbon limited conditions for pH between 7.05 and 7.61. More recently, Erickson et al. (1987) modeled the growth rate of the cyanobacteria *Spirulina platensis* under light and inorganic carbon limited conditions using the Monod model. Table 3 indicates that the parameters they reported for *S.platensis* agree well with those obtained in the present study for *A.variabilis*. Note that Erickson et al. (1987) expressed the Monod model only in terms of HCO_3^- concentration as opposed to C_{TOT}. However, it is equivalent to using C_{TOT} as the pH was kept constant and equal to 9.2. Then, the ratio of HCO_3^- to $H_2CO_3^*$ concentrations is about 800 while CO_3^{2-} concentration is negligibly small. In other words, at pH 9.2, C_{TOT} is approximately equal to the HCO_3^- concentration. In the present study, the pH varies from 6.6 to 7.4 and the ratio of HCO_3^- to $H_2CO_3^*$ concentration varies between 2 and 12. Therefore, both species need to be accounted for in computing C_{TOT} to be used in Equation (2). Furthermore, the aforementioned studies did not account for the inhibitory effect of dissolved inorganic carbon (i.e., $K_I = \infty$) as the concentration of inorganic carbon was low, $C_{TOT} < 0.67 \times 10^{-3}$ kmol C/m^3. However, in the present study, the inorganic carbon concentration reached up to $C_{TOT} < 20 \times 10^{-3}$ kmol

C/m^3 and ignoring the carbon inhibition effects in Equation (2) resulted in poor model predictions. The values of the retrieved parameters μ_{max}, K_G, and K_C agree with those reported by Erickson et al. (1987) and are valid for low carbon concentrations. In addition, the inhibitory effect of large inorganic carbon concentration is successfully accounted for by the modified Monod model through the parameter K_I.

Moreover, due to the fact that CO_2 consumption and O_2 production are mainly growth related processes, their evolution has been successfully modeled using the specific growth rates. On the other hand, H_2 evolution is a much more complex process. It depends on the active enzyme concentration, the O_2 concentration in the medium, the irradiance, as well as the growth rate. Therefore, simple models similar to Equations (6) or (7) could not model all data within $\pm$30%.

Furthermore, these models assume that the irradiance within the culture and the concentration of the dissolved inorganic carbon are known while they cannot be measured directly. Consequently, in the second part of this paper a new analysis for CO_2 consumption, cyanobacterial growth, as well as hydrogen and oxygen productions as functions of $t_{1/2}$ has been developed. Experimental data indicates that $t_{1/2}$ is a relevant time scale for CO_2 consumption, growth, H_2 and O_2 production. The simplicity of this analysis resides in the fact that it depends on directly measurable and controllable quantities. Furthermore, it can be used to determine the light saturation of photosynthesis as shown in Figure 4. However, the applicability of this scaling analysis is limited to systems having (i) the same initial cyanobacteria concentration and (ii) similar pH.

Moreover, Figure 8(a) establishes that an optimum $x_{CO_2,g,o}$ around 0.05 exists for maximum average specific growth rate for all irradiances. Moreover, it shows that the average specific growth rate increases with increasing irradiance. Yoon et al. (2002) reported that for experiments conducted at 30^{o}C with $x_{CO_2,g,o}$ around 0.11 the average specific growth rate decreased from 0.054 to 0.046 h^{-1} for *A.variabilis* as the irradiance increased from 3,500 to 7,000 lux. In the present study at 24^{o}C with initial CO_2 mole fraction of 0.11, μ_{avg} increased from 0.028 to 0.038 h^{-1} for the same increase in irradiance. The observed discrepancy between the results reported in this study and those reported by Yoon et al. (2002) can be attributed to the combination of the differences in pH and in temperature.

Furthermore, Figure 8(b) shows that the average specific CO_2 uptake rate exhibits similar trends to those of the average specific growth rate with an optimum $x_{CO_2,g,o}$ around 0.05 for maximum ψ_{CO_2}. Yoon et al. (2002) reported an average specific CO_2 uptake rate ψ_{CO_2} of about 0.130 kg CO_2/kg dry cell/h for $x_{CO_2,g,o}$ around 0.05 and irradiance around 4,000 lux, whereas, in the present study, it was only 0.060 kg CO_2/kg dry cell/h under the same irradiance and $x_{CO_2,g,o}$. The difference can be attributed to the fact that the experiments of the present study were conducted at 24^{o}C instead of 30^{o}C (Yoon et al., 2002). It is apparent that increasing the temperature enhances the CO_2 uptake metabolism of *A.variabilis* as confirmed by Tsygankov, Borodin, Rao and Hall (1999). Note that due to experimental difficulties in capturing fast CO_2 consumption rate with the available equipment and procedure, no experiments were conducted for initial CO_2 mole fraction less than 0.08 at irradiances higher than 5,000 lux.

Figure 9 and 10 show that H_2 and O_2 concentrations in the headspace increases exponentially during the growth phase. Due to the presence of nitrate in the medium (initially about 20 mM), the nitrogenase activity is expected to be low (Madamwar et al., 2000). Moreover, H_2 production using the nitrogenase enzyme is not expected to stop when the growth stops or slows down such as during two stage H_2 production (Yoon et al., 2002). However, increased concentration of evolved O_2 could have inhibited H_2 production. In addition, the initial anaerobic conditions promotes the bidirectional hydrogenase activity. Therefore, the observed H_2 production during the experiments is expected to be due to the bidirectional hydrogenase activity. Furthermore, the decrease in the H_2 concentration for $t/t_{1/2}$ greater than 1.5 can be attributed to consumption of the produced H_2 due to the presence of uptake hydrogenase (Tsygankov et al., 1998). However, unlike hydrogen, the oxygen concentration does not decrease appreciably beyond the exponential growth phase. Finally, $C_{H_2,g}$ and $C_{O_2,g}$ reach their maximum at dimensionless time $t/t_{1/2}$ equal to 1.37 and 1.55, respectively, and shortly before the CO_2 concentration vanishes at $t/t_{1/2}$ equal to 1.8. Note that the reported values of CO_2, O_2, and H_2 values correspond to the net produced or consumed quantities as it is difficult to experimentally distinguish the contribution of each phenomenon. In particular, CO_2 is being consumed during photosynthesis and being produced during respiration and possibly during H_2 production, provided H_2 production is catalyzed by nitrogenase (Das and Veziroglu,

2001). Similarly, O_2 is being produced during photosynthesis and consumed during respiration.

Figures 11 and 12 show the maximum O_2 and H_2 concentrations attained in the headspace as functions of $x_{CO_2,g,o}$ for different irradiances. Unlike for $C_{O_2,g,max}$, it is difficult to establish a simple and reliable relationship between $C_{H_2,g,max}$ and the parameters G and $x_{CO_2,g,o}$ due to the complexity of the hydrogen metabolism of *A.variabilis*. This complexity arises because (i) the hydrogen production is a strong function of both the irradiance G and the initial CO_2 concentration (Markov, Thomas, Bazin and Hall, 1997a), and (ii) the produced hydrogen is being consumed back by the microorganisms at a rate comparable to the production rate of hydrogen (Tsygankov et al., 1998). Tsygankov et al. (1998) reported that the wild strain *A.variabilis* ATCC 29413 did not produce any hydrogen in the presence of CO_2 in the atmosphere. In contrast, the present study indicates that hydrogen production by the wild strain is possible under argon and CO_2 atmosphere albeit at a lower production rate. Indeed, the maximum hydrogen production observed in our experiments was 0.3 mmol/kg dry cell/h whereas reported rates for wild *A.variabilis* strains range from 5.58 mmol/kg dry cell/h in dark fermentation (Shah, Garg and Madamwar, 2001), 165 mmol/kg dry cell/h in a multi stage photobioreactor (Yoon, Shin, Kim, Sim and Park, 2006), and to 720 mmol/kg dry cell/h under nutritional stress (Sveshnikov et al., 1997). The low hydrogen production rates observed in the present study are attributed to (i) CO_2 fixation and H_2 production processes competing for the reductants generated from water splitting (Prince and Kheshgi, 2005), (ii) the presence of nitrate in the medium (Shah et al., 2001), and (iii) the consumption of the produced H_2 by the wild strain *A.variabilis* at high dissolved O_2 concentrations (Tsygankov et al., 1998).

5 Conclusions

A parametric experimental study has been performed to assess the CO_2 consumption, growth, H_2 and O_2 productions of the cyanobacteria *Anabaena variabilis* ATCC 29413-U^{TM} in batch experiment. The main parameters are the irradiance and the initial CO_2 mole fraction in the headspace. The microorganisms were grown in atmosphere containing argon and CO_2, at a pH of 7.0 $\pm$ 0.4 with nitrate in the medium. A new scaling analysis for CO_2 consumption, growth, and H_2 and

O_2 production is presented. Under the conditions presented in this study, the following conclusions can be drawn for *A.variabilis*,

1. Kinetic equations based on the Monod model are used to model the growth, carbon uptake, and O_2 production by *A.variabilis* taking into account (i) light saturation, (ii) CO_2 saturation, and (iii) CO_2 inhibition. The parameters obtained agree well with values reported for other cyanobacteria (Erickson et al., 1987) at low inorganic carbon concentrations and expands the model to large concentrations when growth inhibition occurs. The experimental data falls within 30% of the model predictions. However, similar approach could not predict experimental data for H_2 production rate.

2. The CO_2 consumption half-time, defined as the time when the CO_2 mole fraction in the gas phase decreases to half of its initial value, is a relevant time scale for CO_2 consumption, growth, H_2 and O_2 production. It depends on the total irradiance incident on the vials and the initial CO_2 mole fraction.

3. The scaling analysis facilitates the determination of the saturation irradiance which is found to be 5,170 lux.

4. For maximum specific CO_2 consumption and specific growth rates, the optimum initial CO_2 mole fraction in the gas phase is about 0.05 for any irradiance between 1,000 and 16,000 lux.

5. Optimum irradiance for maximum H_2 production has been found to be around 10,000 lux despite the low overall H_2 production rates.

6. Neither the CO_2 consumption nor the growth rate was inhibited by irradiance up to about 16,000 lux.

Finally, the kinetic equations can be used in simulations for optimizing the operating conditions of a photobioreactor for rapid growth and maximum CO_2 mitigation. Moreover, it is expected that the above experimental and scaling analysis method can be used for analyzing other CO_2 mitigating and H_2 producing microorganisms.

Acknowledgements

The authors gratefully acknowledge the support of the California Energy Commission through the Energy Innovation Small Grant (EISG 53723A/03-29; Project Manager: Michelle McGraw). They are indebted to Chu Ching Lin, Edward Ruth, Jong Hyun Yoon, and Dr. James C. Liao for their helpful discussions and exchanges of information.

References

Asenjo, J. and Merchuk, J. (1995). *Bioreactor System Design*, Marcel Dekker, New York, NY.

Badger, M. and Andrews, T. (1982). Photosynthesis and inorganic carbon usage by the marine cyanobacterium *Synechococcus sp.*, *Plant Physiol* **70**: 517–523.

Benemann, J. (2000). Hydrogen production by microalgae, *J Appl Phycol* **12**: 291–300.

Benjamin, M. (2002). *Water Chemistry*, McGraw Hill, New York, NY.

Berberoğlu, H. and Pilon, L. (2007). Experimental measurement of the radiation characteristics of hydrogen producing microorganisms, *Fifth International Symposium on Radiative Transfer, Bodrum, Turkey, June 17-22*.

Berberoğlu, H., Yin, J. and Pilon, L. (2007). Simulating light transfer in a bubble sparged photobioreactor for simultaneous hydrogen fuel production and CO_2 mitigation, *Int J Hydrogen Energy, (in press)*.

Borodin, V., Tsygankov, A., Rao, K. and Hall, D. (2000). Hydrogen production by A*nabaena* variabilis PK84 under simulated outdoor conditions, *Biotechnol Bioeng* **69**: 478–485.

Das, D. and Veziroglu, T. (2001). Hydrogen production by biological processes: a survey of literature, *Int J Hydrogen Energy* **26**: 13–28.

Dunn, I., Heinzle, E., Ingham, J. and Prenosil, J. (2003). *Biological reaction engineering; dynamic modelling fundamentals with simulation examples. Second Edition*, Wiley-VCH.

Erickson, L., Curless, C. and Lee, H. (1987). Modeling and simulation of photosynthetic microbial growth, *Ann NY Acad Sci* **506**: 308–324.

Goldman, J., Oswald, W. and Jenkins, D. (1974). The kinetics of inorganic carbon limited algal growth, *Water Pollut Control Fed* **46**: 554–574.

Hansel, A. and Lindblad, P. (1998). Towards optimization of cyanobacteria as biotechnologically relevant producers of molecular hydrogen, a clean and renewable energy souce, *Appl Microbiol Biotechnol* **50**: 153–160.

Happe, T., Schutz, K. and Bohme, H. (2000). Transcriptional and mutational analysis of the uptake hydrogenase of the filamentous cyanobacterium Anabaena variabilis ATCC 29413, *J Biotechnol* **182**: 1624–1631.

Madamwar, D., Garg, N. and Shah, V. (2000). Cyanobacterial hydrogen production, *World J Microbiol Biotechnol* **16**(8-9): 757–767.

Markov, S., Bazin, M. and Hall, D. (1995). Hydrogen photoproduction and carbon dioxide uptake by immobilized A*nabaena variabilis* in a hollow-fiber photobioreactor, *Enzyme Microb Technol* **17**: 306–310.

Markov, S., Lichtl, R., Rao, K. and Hall, D. (1993). A hollow fibre photobioreactor for continuous production of hydrogen by immobilized cyanobacteria under partial vacuum, *Int J Hydrogen Energy* **18**: 901–906.

Markov, S., Thomas, A., Bazin, M. and Hall, D. (1997a). Photoproduction of hydrogen by cyanobacteria under partial vacuum in batch culture or in a photobioreactor, *Int J Hydrogen Energy* **22**: 521–524.

Markov, S., Weaver, P. and Seibert, M. (1997b). Spiral tubular bioreactors for hydrogen production by photosynthetic microorganisms - design and operation, *Appl Biochem Biotechnol* **63-65**: 577–584.

Merzlyak, M. and Naqvi, K. (2000). On recording the true absorption spectrum and scattering spectrum of a turbid sample: application to cell suspensions of cyanobacterium Anabaena variabilis, *J Photochem Photobiol B* **58**: 123–129.

of Energy, D. (Accessed on: April 19, 2007). Joint Genome Institute, http://www.jgi.doe.gov.

Pinto, F., Troshina, O. and Lindblad, P. (2002). A brief look at three decades of research on cyanobacterial hydrogen evolution, *Int J Hydrogen Energy* **27**: 1209–1215.

Prince, R. C. and Kheshgi, H. S. (2005). The photobiological production of hydrogen: potential efficiency and effectiveness as a renewable fuel, *Crit Rev Microbiol* **31**: 19–31.

Shah, V., Garg, N. and Madamwar, D. (2001). Ultrastructure of the fresh water cyanobacterium A*nabaena variabilis* SPU 003 and its application for oxygen-free hydrogen production, *FEMS Microbiol Lett* **194**: 71–75.

Smith, L., McCarthy, P. and Kitanidis, P. (1998). Spreadsheet method for evaluation of biochemical reaction rate coefficients and their uncertainties by weighted nonlinear least-squares analysis of the integrated monod equation, *Appl Environ Microbiol* **64**: 2044–2050.

Sveshnikov, D., Sveshnikova, N., Rao, K. and Hall, D. (1997). Hydrogen metabolism of mutant forms of A*nabaena variabilis* in continuous cultures and under nutritional stress, *FEMS Microbiol Lett* **147**: 297–301.

Tsygankov, A., Borodin, V., Rao, K. and Hall, D. (1999). H_2 photoproduction by batch culture of A*nabaena variabilis* ATCC 29413 and its mutant PK84 in a photobioreactor, *Biotechnol Bioeng* **64**: 709–715.

Tsygankov, A., Fedorov, A., Kosourov, S. and Rao, K. (2002). Hydrogen production by cyanobacteria in an automated outdoor photobioreactor under aerobic conditions, *Biotechnol Bioeng* **80**: 777–715.

Tsygankov, A., Serebryakova, L., Rao, K. and Hall, D. (1998). Acetylene reduction and hydrogen photoproduction by wild-type and mutant strains of A*nabaena* at different CO_2 and O_2 concentrations, *FEMS Microbiol Lett* **167**: 13–17.

Yoon, J., Shin, J., Kim, M., Sim, S. and Park, T. (2006). Evaluation of conversion efficiency of light to hydrogen energy by A*nabaena variabilis*, *Int J Hydrogen Energy* **31**: 721–727.

Yoon, J., Sim, S., Kim, M. and Park, T. (2002). High cell density culture of Anabaena variabilis using repeated injections of carbon dioxide for the production of hydrogen, *Int J Hydrogen Energy* **27**: 1265–1270.

Table 1: Summary of experimental conditions used and associated maximum specific growth, CO_2 consumption and H_2 production rates reported in the literature using various strains of *Anabaena variabilis*.

	Stage I			Stage II			Maximum Reported Rates			
***A.variabilis* Strain**	**Gas Phase**	**Medium**	**Irradiance (lux)**	**Gas Phase**	**Medium**	**Irradiance (lux)**	μ	$\psi_{\mathbf{CO_2}}$	$\pi_{\mathbf{H_2}}$	**Ref.**
Kutzing 1403/4B	95 vol.% Air + 5 vol.% CO_2	Allen and Arnon w/o Nitrate at 25^{o}C	1,800	300 mm Hg Vacuum	Same as Stage I	13,000	N/A	7,000	830	(Markov, Bazin and Hall, 1995)
ATCC 29413	89 vol.% Air + 11 vol.% CO_2	BG-11$_o$ + 3.5 mM $NaNO_3$ at 30^{o}C	2,500 to 5,500	Argon	BG-11$_o$ w/o Nitrate at 30^{o}C	9,000 to 12,000	0.05	2,700	80	(Yoon et al., 2002)
ATCC 29413	98 vol.% Air + 2 vol.% CO_2	Allen and Arnon w/o Nitrate Molybdenum replaced w/ Vanadium at 30^{o}C	8,000	Argon	Same as Stage I	10,000 to 14,000	N/A	N/A	630	(Tsygankov et al., 1998)
PK 84	98 vol.% Air + 2 vol.% CO_2	Allen and Arnon w/o Nitrate Molybdenum replaced w/ Vanadium at 30^{o}C	8,000	Argon	Same as Stage I	10,000 to 14,000	N/A	N/A	515	(Tsygankov et al., 1998)
ATCC 29413	73 vol.% Ar + 25 vol.% N_2 + 2 vol.% CO_2	Allen and Arnon w/o Nitrate Molybdenum replaced w/ Vanadium at 30^{o}C	6,500	93 vol.% Ar + 5 vol.% N_2 + 2 vol.% CO_2	Same as Stage I	6,500	N/A	N/A	720.37	(Sveshnikov et al., 1997)
PK 84	73 vol.% Ar + 25 vol.% N_2 + 2 vol.% CO_2	Allen and Arnon w/o Nitrate Molybdenum replaced w/ Vanadium at 30^{o}C	6,500	93 vol.% Ar + 5 vol.% N_2 + 2 vol.% CO_2	Same as Stage I	6,500	N/A	N/A	2,600	(Sveshnikov et al., 1997)
PK 84	98 vol.% Air + 2 vol.% CO_2	Allen and Arnon w/o Nitrate Molybdenum replaced w/ Vanadium at 30^{o}C	outdoor	98 vol.% Air + 2 vol.% CO_2	Same as Stage I	outdoor	0.03	N/A	300	(Tsygankov et al., 2002)

Table 2: Summary of the parameters used in the experiments.

Label	**G** (lux)	$x_{CO_2,g,o}$	$\mathbf{t}_{1/2}$ (h)	μ_{avg} (1/h)	Y_{X/CO_2} (kg/kg)	ψ_{CO_2} (kg/kg/h)
0GH	7000	0.20	74.4	0.024	0.373	0.065
0IJ	14700	0.20	65.3	0.028	0.352	0.081
1AB	1120	0.15	232.8	0.009	0.451	0.020
1CD	1680	0.15	189.3	0.013	0.589	0.023
1EF	3950	0.15	82.3	0.024	0.465	0.051
1GH	8700	0.15	49.5	0.033	0.398	0.082
1IJ	16100	0.15	46.8	0.036	0.381	0.094
2AB	1175	0.08	120.6	0.013	0.555	0.024
2CD	1820	0.08	98.4	0.016	0.626	0.026
2EF	4300	0.08	53.2	0.027	0.489	0.055
2GH	8000	0.08	37.1	0.038	0.440	0.086
2IJ	16100	0.08	39.1	0.041	0.433	0.094
3AB	1195	0.04	71.4	0.018	0.685	0.026
3CD	1815	0.04	57.3	0.022	0.755	0.030
3EF	4190	0.04	32.0	0.037	0.629	0.059
4AB	1265	0.03	64.9	0.017	0.840	0.020
4CD	2430	0.03	73.8	0.023	0.859	0.026
4EF	4600	0.03	27.3	0.029	0.748	0.038

Table 3: Summary of the parameters used in kinetic modeling of *A.variabilis*.

Parameter	**Present Study**	**Erickson et al. (1987)**	**Equation**
μ_{max} (1/h)	0.10	0.12	2
K_G (lux)	4440	4351	2
K_C (kmol C /m^3)	0.0002	0.0002	2
K_I (kmol C /m^3)	0.0182	N/A	2
$Y_{X/C}$ (kg dry cell/kmol C)	24.96	25.18	6
$Y_{O_2/X}$ (kg O_2/kg dry cell)	1.28	N/A	7

List of Figures

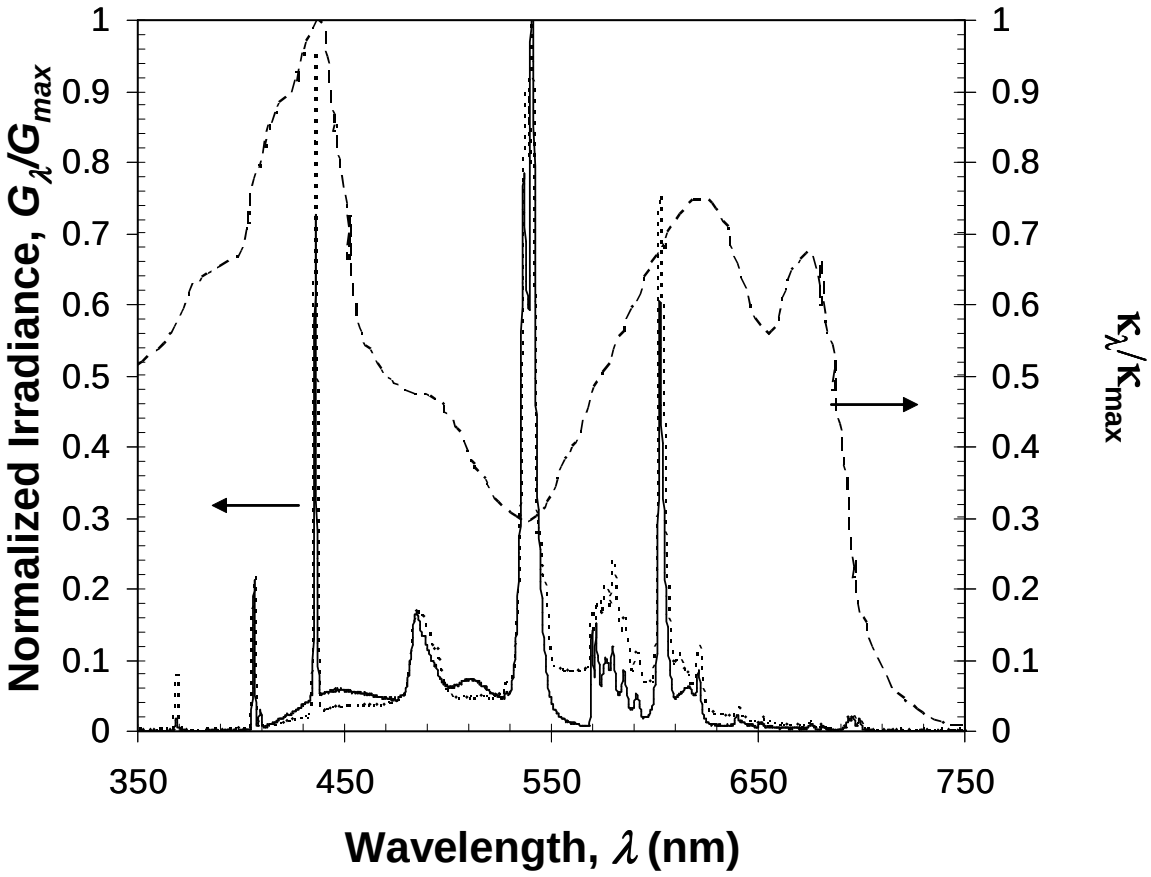

Figure 1: The normalized spectral irradiance of Ecologic (solid line) and Fluorex (dotted line) light bulbs G_λ/G_{max} along with the normalized absorption coefficient of *A.variabilis* (dashed line) $\kappa_\lambda/\kappa_{max}$ (Merzlyak and Naqvi 2000).

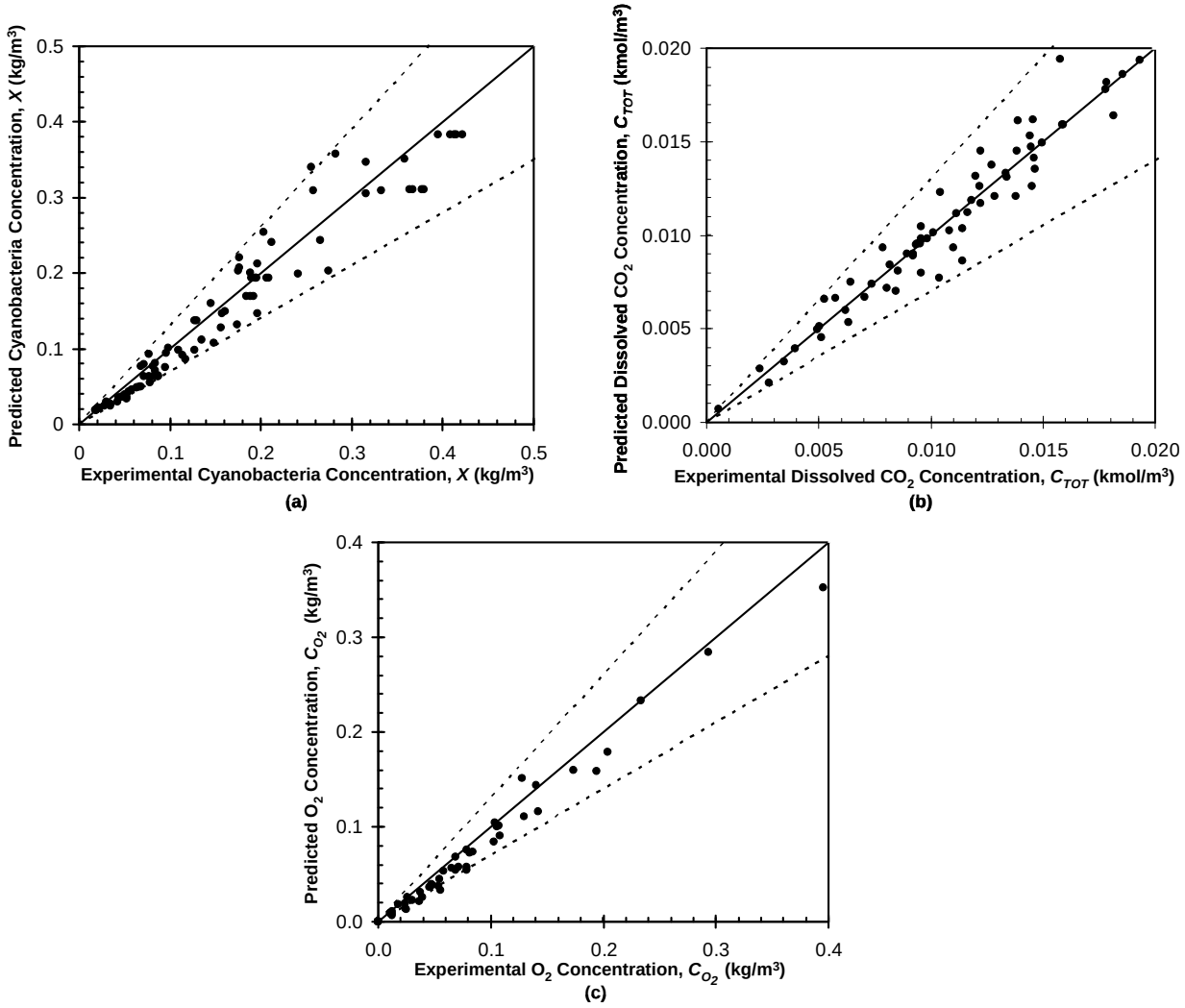

Figure 2: Comparison between experimental data and kinetic model predictions for (a) cyanobacterial concentration [Equation (2)], (b) total dissolved inorganic carbon concentration [Equation (6)], and (c) total O_2 concentration [Equation (7)]. The dashed lines correspond to $\pm 30\%$ deviation from model predictions.

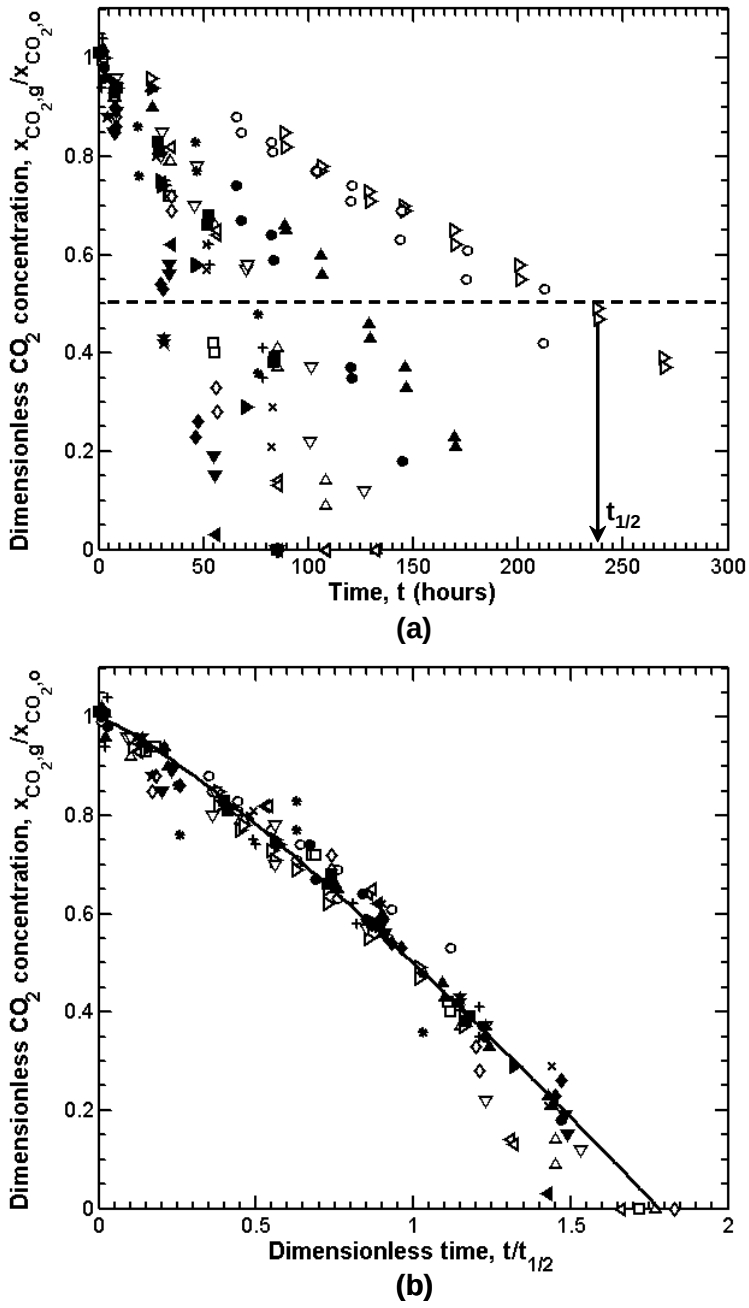

Figure 3: (a) Normalized CO_2 consumption data versus time, (b) Normalized CO_2 consumption data versus dimensionless time for (△) 0GH, (◁) 0IJ, (▷) 1AB, (○) 1CD, (▽) 1EF, (□) 1GH, (♢) 1IJ, (▲) 2AB, (●) 2CD, (▶) 2EF, (▼) 2GH, (◀) 2IJ, (■) 3AB, (×) 3CD, (⧫) 3EF, (+) 4AB, (∗) 4CD, (⋆) 4EF. The solid line corresponds to $x_{CO_2,g}/x_{CO_2,g,o} = 1 - 0.5(t/t_{1/2})^{1.2}$.

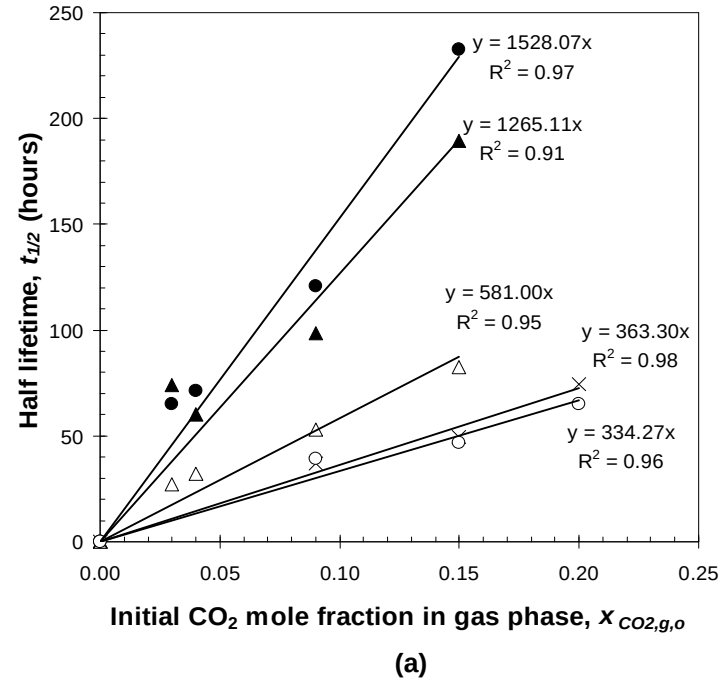

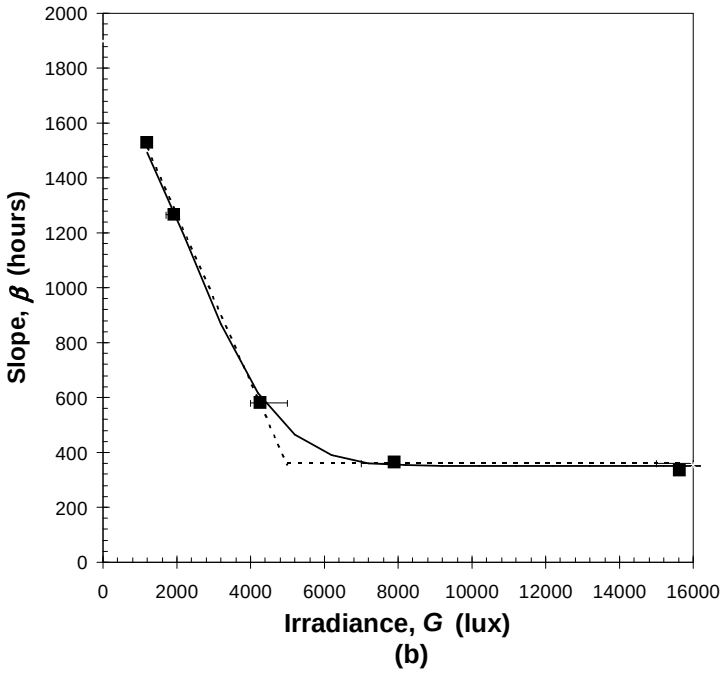

Figure 4: (a) Half-time as a function of $x_{CO_2,g,o}$ for (●) 1,100-1,200 lux, (▲) 1,700-1,800 lux, (△) 4,000-5,000 lux, (×) 7,000-8,000 lux, and (○) 15,000-16,000 lux. (b) Slope β as a function of irradiance G. The solid line corresponds to $\beta = 350 + 1300\exp(-9 \times 10^{-8} G^2)$.

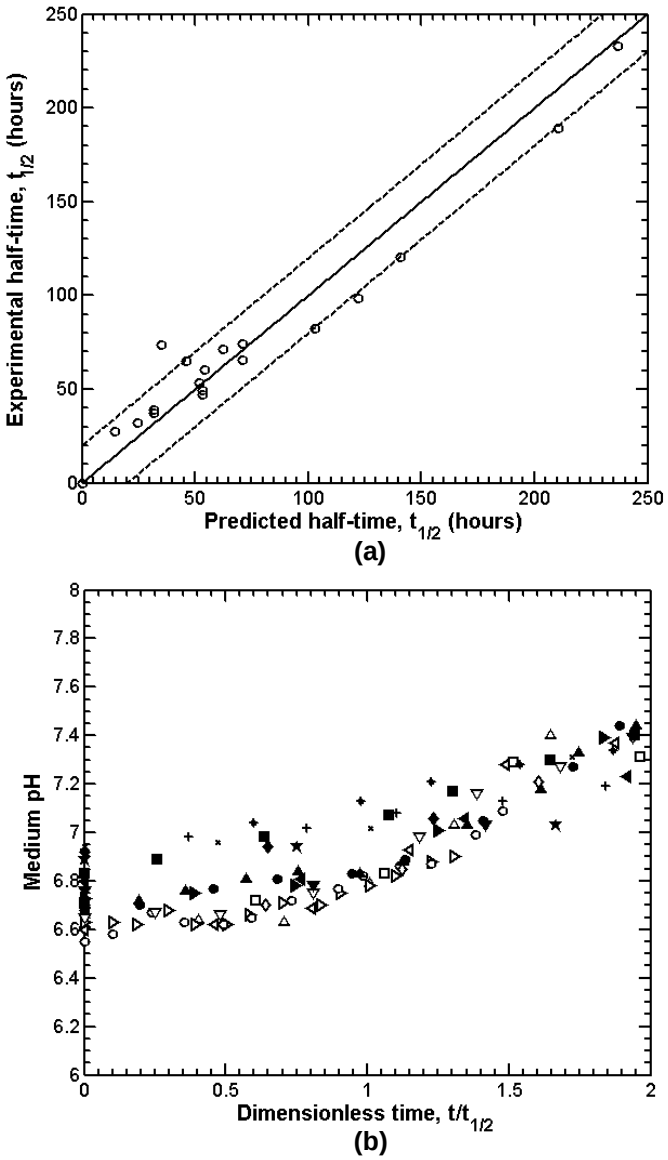

Figure 5: (a) Comparison of experimental versus predicted half-times. The solid line corresponds to the model $t_{1/2} = (1900 - 0.3G)x_{CO_2,g,o}$ and the dashed lines correspond to $\pm$20 hour deviations from the model. (b) The medium pH as a function of the dimensionless time $t/t_{1/2}$ for ($\triangle$) 0GH, ($\triangleleft$) 0IJ, ($\triangleright$) 1AB, ($\circ$) 1CD, ($\triangledown$) 1EF, ($\square$) 1GH, ($\Diamond$) 1IJ, ($\blacktriangle$) 2AB, ($\bullet$) 2CD, ($\blacktriangleright$) 2EF, ($\blacktriangledown$) 2GH, ($\blacktriangleleft$) 2IJ, ($\blacksquare$) 3AB, ($\times$) 3CD, ($\blacklozenge$) 3EF, ($+$) 4AB, ($*$) 4CD, ($\star$) 4EF.

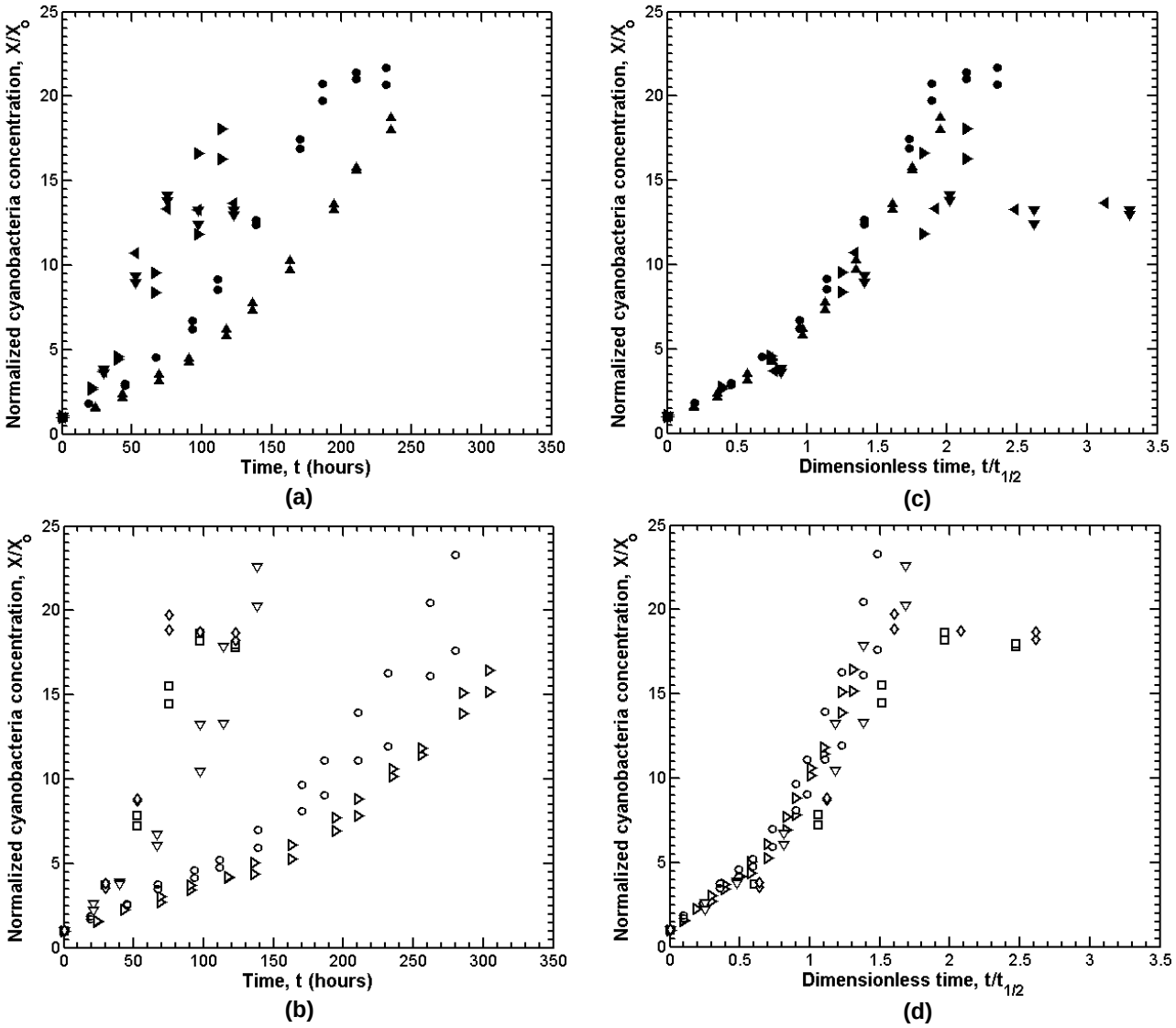

Figure 6: Normalized cyanobacteria concentrations at all irradiances as functions of time for (a) $x_{CO_2,g,o} = 0.08$ and (b) $x_{CO_2,g,o} = 0.15$. Normalized cyanobacteria concentrations at all irradiances as functions of dimensionless time for (c) $x_{CO_2,g,o} = 0.08$ and (d) $x_{CO_2,g,o} = 0.15$ for (▲) 2AB, (●) 2CD, (►) 2EF, (▼) 2GH, (◄) 2IJ, (▷) 1AB, (○) 1CD, (▽) 1EF, (□) 1GH, (◊) 1IJ.

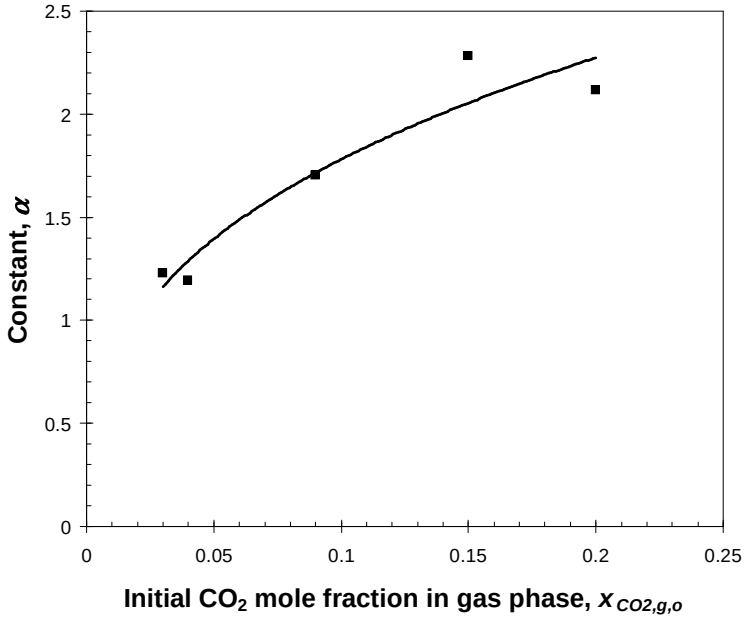

Figure 7: (a) The constant α in Equation (10) as a function of $x_{CO_2,g,o}$. The solid line corresponds to $\alpha = 4x_{CO_2,g,o}^{0.35}$.

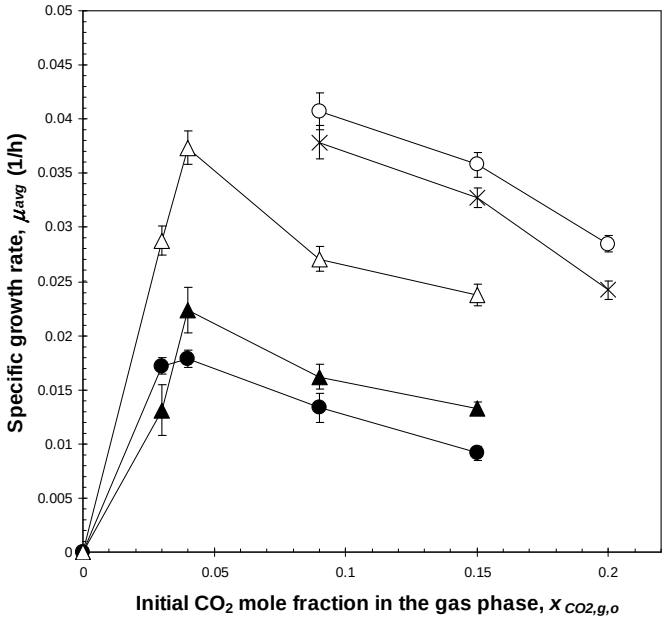

(a)

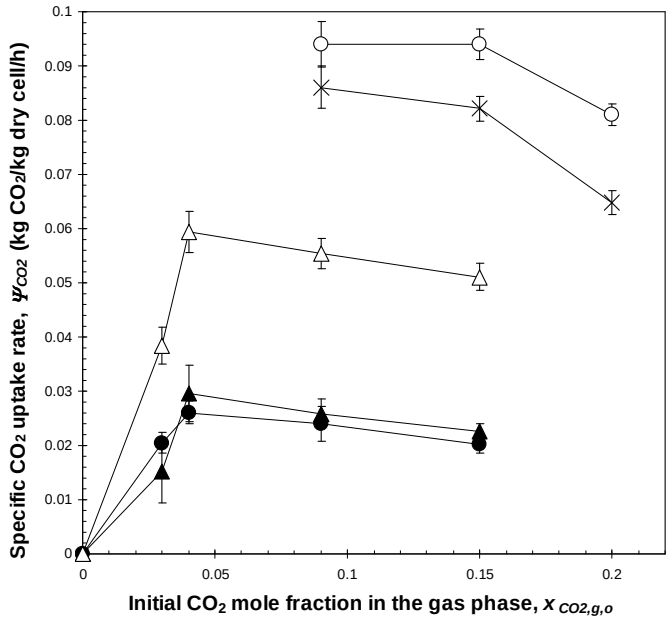

(b)

Figure 8: (a) The average specific growth rate μ_{avg}, and (b) the average specific CO_2 uptake rate ψ_{CO_2} of *A.variabilis* as functions of $x_{CO_2,g,o}$ at all irradiances: (●) 1,100-1,200 lux, (▲) 1,700-1,800 lux, (△) 4,000-5,000 lux, (×) 7,000-8,000 lux, and (○) 15,000-16,000 lux.

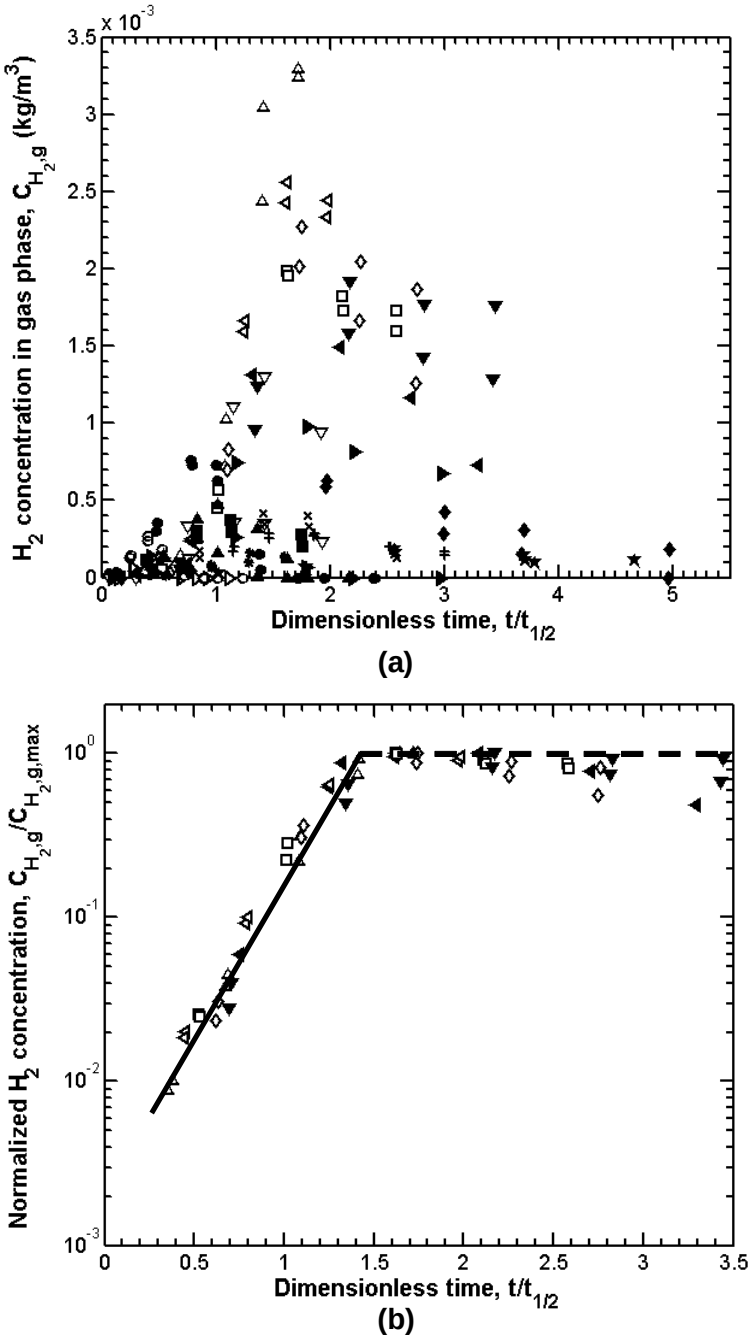

Figure 9: Concentration of hydrogen accumulated in the head-space (a) for all tests versus dimensionless time $t/t_{1/2}$, (b) normalized with the maximum concentration produced versus dimensionless time $t/t_{1/2}$ for irradiance $G \geq$ 7,000 lux. The solid line corresponds to $C_{H_2,g}/C_{H_2,g,max} = \exp[4.45(t/t_{1/2}) - 6.1]$.(△) 0GH, (◁) 0IJ, (▷) 1AB, (○) 1CD, (▽) 1EF, (□) 1GH, (◊) 1IJ, (▲) 2AB, (●) 2CD, (►) 2EF, (▼) 2GH, (◄) 2IJ, (■) 3AB, (×) 3CD, (⧫) 3EF, (+) 4AB, (∗) 4CD, (⋆) 4EF.

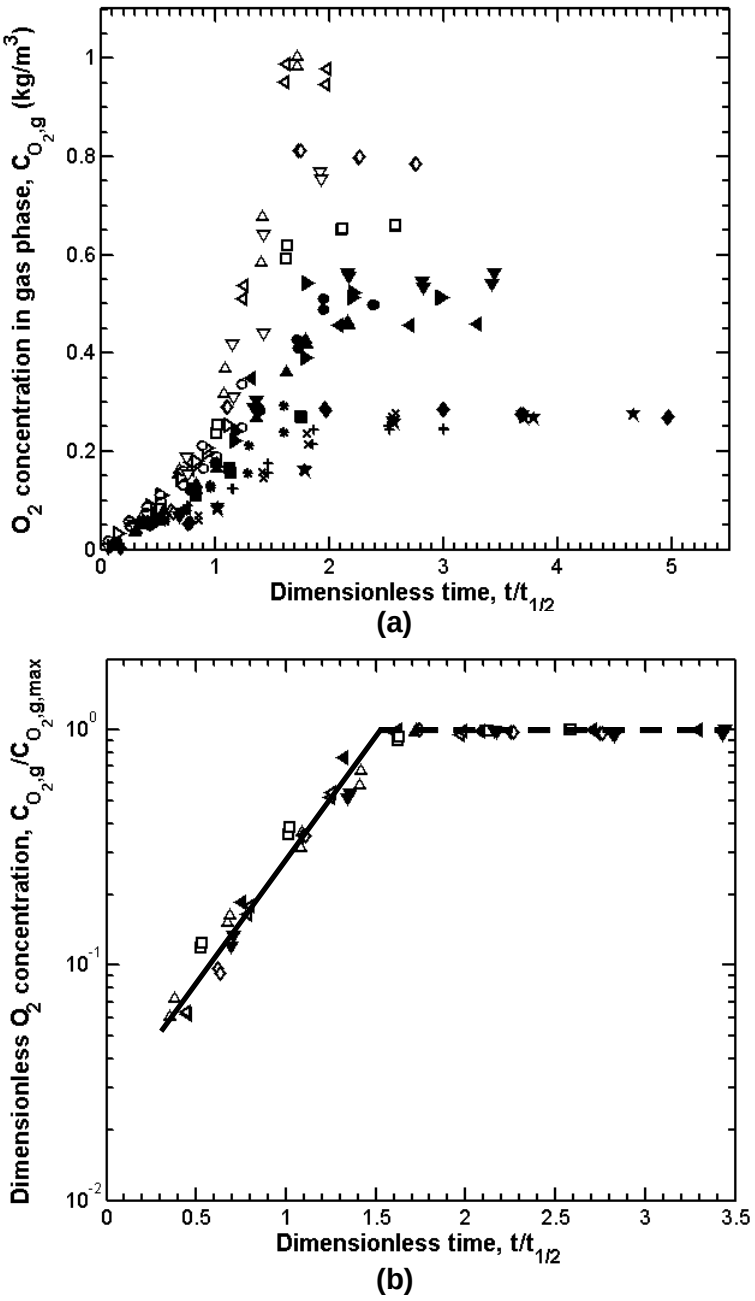

Figure 10: Concentration of oxygen accumulated in the head-space for (a) all tests versus dimensionless time $t/t_{1/2}$, (b) normalized with the maximum concentration produced versus dimensionless time $t/t_{1/2}$ for irradiance $G \geq$ 7,000 lux. The solid line corresponds to $C_{O_2,g}/C_{O_2,g,max} = \exp[2.25(t/t_{1/2}) - 3.5]$. (△) 0GH, (◁) 0IJ, (▷) 1AB, (○) 1CD, (▽) 1EF, (□) 1GH, (◇) 1IJ, (▲) 2AB, (●) 2CD, (►) 2EF, (▼) 2GH, (◄) 2IJ, (■) 3AB, (×) 3CD, (♦) 3EF, (+) 4AB, (∗) 4CD, (⋆) 4EF.

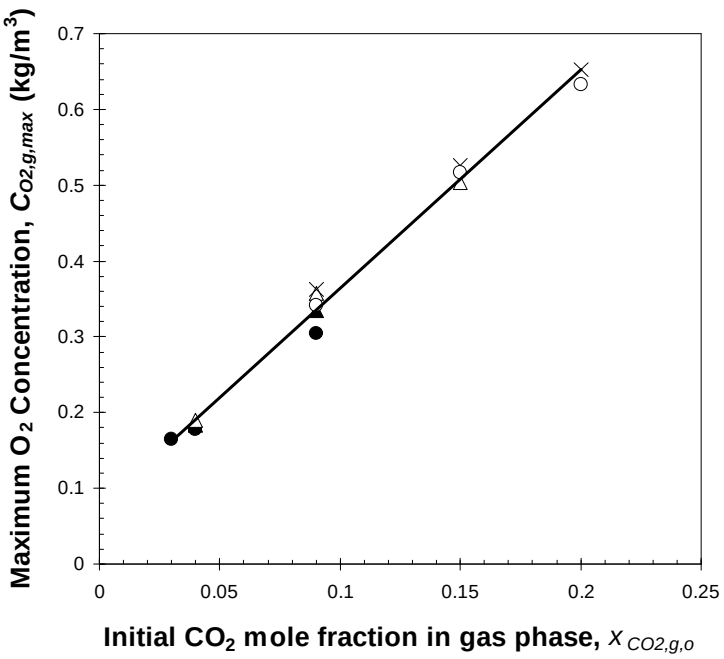

Figure 11: Maximum concentration of oxygen accumulated in the head-space $C_{O_2,max}$ as a function of the $x_{C_{CO_2},g,o}$ for (●) 1,100-1,200 lux, (▲) 1,700-1,800 lux, (△) 4,000-5,000 lux, (×) 7,000-8,000 lux, and (○) 15,000-16,000 lux. The solid line corresponds to $C_{O_2,g,max} = 3.45 x_{CO_2,g,o}$.

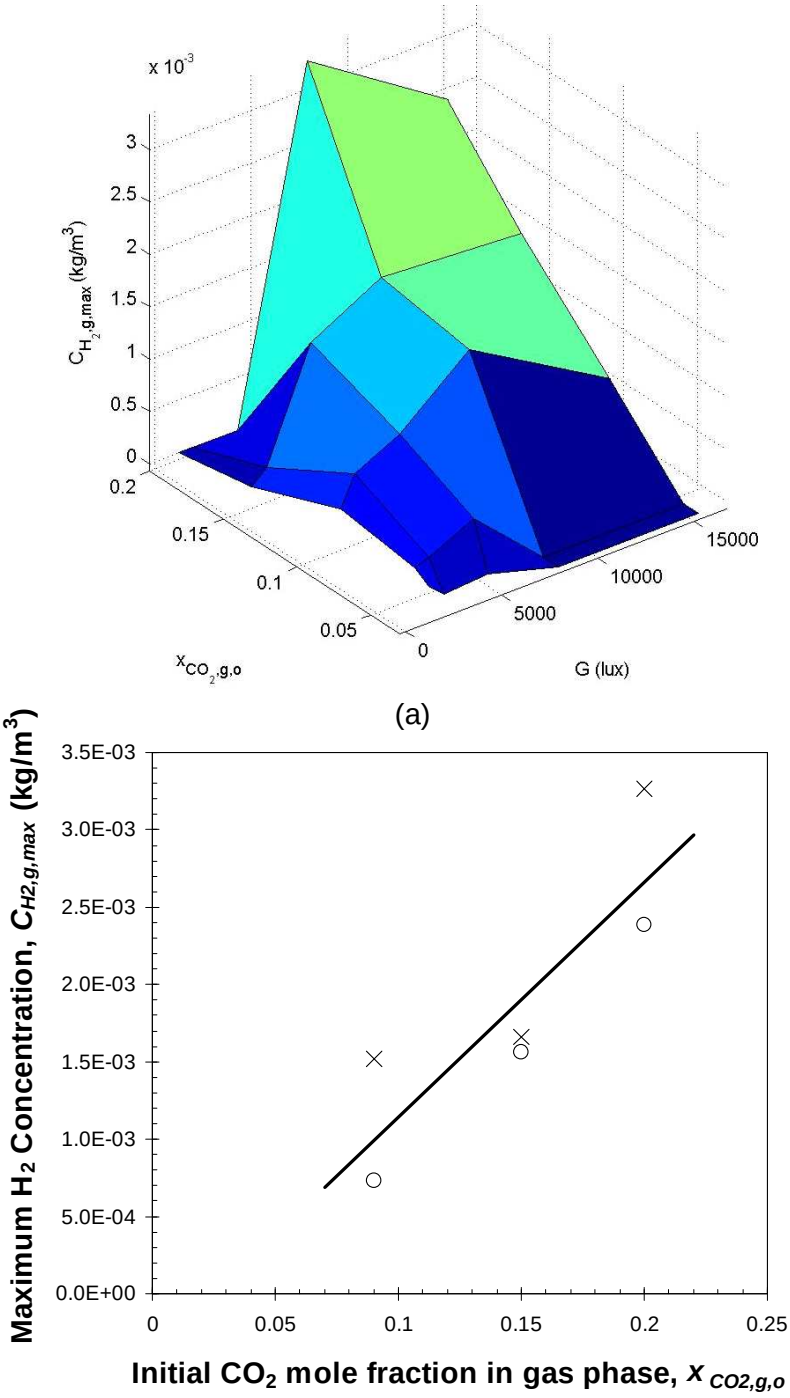

Figure 12: (a) Maximum concentration of hydrogen accumulated in the head-space as a function of the initial CO_2 mole fraction and irradiance. (b) $C_{H_2,max}$ as a function of $x_{C_{CO_2},g,o}$ for two of the highest irradiances for ($\times$) 7,000-8,000 lux, and ($\circ$) 15,000-16,000 lux. The solid line corresponds to $C_{H_2,g,max} = 1.50 \times 10^{-2} x_{CO_2,g,o} - 3.75 \times 10^{-4}$.